Atmos. Chem. Phys. Discuss., 10, 27227–27253, 2010
www.atmos-chem-phys-discuss.net/10/27227/2010/
doi:10.5194/acpd-10-27227-2010

Atmospheric Chemistry and Physics Discussions

Concurrent observations of atomic iodine, molecular iodine and ultrafine particles in a coastal environment

A. S. Mahajan[1], M. Sorribas[2], J. C. Gómez Martín[1], S. M. MacDonald[3], M. Gil[2], J. M. C. Plane[3], and A. Saiz-Lopez[1]

[1]Laboratory for Atmospheric and Climate Science (CIAC), CSIC, Toledo, Spain
[2]Atmospheric Research and Instrumentation Branch, National Institute for Aerospace and Technology (INTA), Huelva, Spain
[3]School of Chemistry, University of Leeds, Leeds, UK

Received: 3 November 2010 – Accepted: 7 November 2010 – Published: 10 November 2010

Correspondence to: A. Saiz-Lopez (a.saiz-lopez@ciac.jccm-csic.es)

Published by Copernicus Publications on behalf of the European Geosciences Union.

Abstract

Simultaneous measurements of atomic iodine (I), molecular iodine (I_2) and ultrafine particles were made at O Grove, Galicia (42.50° N, 8.87° W), on the northwest coast of Spain. The observations show a strong tidal signature, and indicate that the most probable sources of reactive iodine species are the exposed macroalgae during low tide. For the first time, I_2 and I were concurrently measured revealing a high average I_2/I ratio of ~32, which is higher than previously inferred by modelling studies. A 1-dimensional photochemical model is employed to simulate the observations showing that the high I_2/I ratio can be reproduced in the presence of fast vertical mixing close to the surface, or using an extra chemical loss for I atoms with an unknown species. There is a lack of strong correlation between the I_2/I and ultrafine particles, indicating that although they both have macroalgal sources, these were not at the same location. The model simulations also suggest that the source of the observed ultrafine particles is likely not very close to the measurement site, in order for the particles to form and grow, but the source for I and I_2 must be local. Finally, the effect of NO_x levels on iodine oxides, and the conditions under which iodine particle bursts will be suppressed, are explored.

1 Introduction

Measurements of reactive iodine species (RIS) in the marine boundary layer (MBL) were initiated by the detection of iodine monoxide (IO) (Alicke et al., 1999), iodine dioxide (OIO) (Allan et al., 2001) and I_2 (Saiz-Lopez and Plane, 2004). Recently, the positive detection of I atoms has also been reported (Bale et al., 2008). The above RIS affect the MBL oxidising capacity through depletion of ozone (Chameides and Davis, 1980; Davis et al., 1996; Vogt et al., 1996), and changing the HO_2/OH and NO_2/NO balance (McFiggans et al., 2000; Bloss et al., 2005; Saiz-Lopez et al., 2008).

ACPD
10, 27227–27253, 2010

In the coastal marine environment, emissions of I_2 from exposed macroalgae, such as *Laminaria digitata* and *Laminaria hyperborea* (McFiggans et al., 2004; Ball et al., 2010), have been shown to be the main source of RIS, resulting in an anti-correlation with tidal height. Measurements of I_2 have so far been reported at three different mid-latitudinal coastal locations: Mace Head, Ireland (Saiz-Lopez and Plane, 2004; Peters et al., 2005; Huang et al., 2010), California, USA (Finley and Saltzman, 2008) and Roscoff, France (Leigh et al., 2009; Mahajan et al., 2009). However, detection of I atoms has only been reported by Bale et al. (2008) at Mace Head.

Iodine oxides have also been implicated in ultrafine aerosol formation in coastal environments (O'Dowd et al., 2004; McFiggans, 2005). However, iodine-induced ultrafine particle formation has only been reported to occur in two locations so far, i.e. Mace Head, Ireland (O'Dowd et al., 2002; McFiggans et al., 2004) and Roscoff, France (McFiggans et al., 2010). The exact mechanism for particle formation is still not well understood, although the latest laboratory results suggest that IO and OIO recombine leading to the formation of I_2O_3 and I_2O_4, and these two species are directly involved in further polymerisation and growth to ultrafine particles (Saunders et al., 2010).

In this paper we present simultaneous observations of I_2, I and ultrafine particles in a semi-polluted coastal environment, and use these observations to test the current knowledge of iodine chemistry.

2 Experimental

Measurements were made at O Grove, Galicia (42.50° N, 8.87° W), on the northwest coast of Spain (Fig. 1) as a part of the Laminariae Emissions in Galicia: Observation by fLuorescence and Absorption Spectroscopy (LEGOLAS) field study, from 30 April to 7 May 2010 . A macroalgae bed, adjacent to the coast and about 30–50 m wide was present between 5–10 m to the north of the measurement site. This area was completely exposed during low tide. Additionally, a similar macroalgal distribution occurs on the south coast of the forested island of Arosa, which is at a distance of ap-

ACPD
10, 27227–27253, 2010

proximately 3.5 km towards the north (Fig. 1). Further to the north, beyond the island of Arosa, the bay concluded at Cabo de Cruz and Rianxo, which were at a distance of 15 km and 20 km, respectively (Fig. 1), although information about any macroalgal distribution around this part of the bay was not available.

2.1 Resonance and Off-resonance Fluorescence by Lamp Excitation (ROFLEX)

Concurrent measurements of I_2 and I were performed using a newly developed instrument based on the detection of molecular and atomic resonance and off-resonance ultraviolet fluorescence excited by lamp emission. The ROFLEX instrument is described in detail in a companion paper (Gómez Martin et al., 2010), and therefore only a brief description will be given here. The core of the instrument is a low pressure chamber where ambient air is drawn at a rate of approximately 5 slm using a rotary vacuum pump. The iodine atoms and molecules contained in the sampled air are excited by VUV radiation emitted by a radiofrequency discharge iodine lamp. Fluorescence is then collected at right angles by two highly sensitive photon-counting modules. The ambient air flow can also be directed first through an iodine trap for a set time interval before being drawn into the fluorescence chamber, thus allowing a measurement of iodine-free background signal. The iodine trap comprised of an opaque PVC tube in which I atoms are scavenged by ambient ozone in the absence of photolysis, and a Peltier-cooled aluminium box where both I and I_2 are frozen out of the flow. Calibration of the molecular fluorescence signal is achieved in the laboratory by Incoherent Broad Band Cavity-enhanced Absorption Spectroscopy (IBBCEAS), whereas the atomic signal is calibrated by the photolysis of known amounts of molecular iodine. During the campaign, the average detection limits for I atoms and I_2 were 2 and 30 pptv (equivalent to pmol mol^{-1}), respectively, corresponding to an integration time of 10 min (5 min air sampling + 5 min background). The instrument was located on the coast, less than 2 m away from the high tide line. The measurement height was 1.5 m above the average sea level.

ACPD
10, 27227–27253, 2010

2.2 Aerosol instrumentation

Continuous particle size measurements were simultaneously carried out by two subsystems monitoring different size ranges of dry particles. Particles number size distribution in the 9–407 nm range was measured using a Scanning Mobility Particle Sizer (SMPS) which comprised of an Electrostatic Classifier (TSI Model 3080) in conjunction with an Ultrafine Condensation Particle Counter (TSI Model 3776) with 5 min time resolution. The polydisperse aerosol flow was 0.6 l min^{-1} and the sheath flow was 6 l min^{-1}; the latter was dried with silica gel in a closed loop. As a result of the different operational flows of the Electrostatic Classifier (0.6 l min^{-1}) and the UCPC (1.5 l min^{-1}), an excess flow of 0.9 l min^{-1} was added before the UCPC inlet using a critical orifice to control the flow. Total concentration for particles larger than 3 nm (50% detection at 3 nm) was measured by a second UCPC (TSI Model 3776) operating at high flow and with 1 min time resolution. Sample flow for both instruments was dried to RH < 30% using a Perma Pure dryer (Perma Pure Inc, Toms River, N) by supplying pressurised dry air to the sheath of the dryer. AIM software (version 8.0.0, TSI INC., St. Paul., MN, USA) was used for data reduction and analysis of the SMPS and UCPC outputs. The accuracy of the system is about 10%. Although the lower size limits for the UCPC are not well defined, the difference in total particle number concentration between the UCPC and SMPS systems is attributed to particles in the size range between 3 and 9 nm (ultrafine particles). The inlet for the particle measurements was located on top of a shipping container, placed 10 m away from the shore line. The height of the inlet was about 3.5 m above the average sea level.

2.3 Ancillary measurements

In addition to the above instruments, observations of O_3 (2B Technologies, dual beam ozone monitor), NO, NO_2 (Teledyne API, 400 EU) at 3.5 m and meteorological data at two different heights of 1.5 m and 3.5 m (Davis VP2 weather stations) were also available.

ACPD
10, 27227–27253, 2010

3 Observations

The entire time series of measurements made during the LEGOLAS campaign is summarised in Fig. 2. The I_2 and I mixing ratios are shown in panels 2a and 2b, respectively. Iodine atoms and molecules were observed above the detection limit on 4 days and 1 night, with relatively high values observed on 30 April and 3 May 2010. The highest mixing ratios observed were 10±5 pptv for I atoms and 350±100 pptv for I_2, both on 30 April. Measurement uncertainties encompass ±2.5 c s^{-1} (counts per second) precision and 20% accuracy for I and ±5 c s^{-1} precision and 22% accuracy for I_2. The precision of the field measurements was found to be ~3 times worse than typical laboratory values, reflecting the temperature instability of the lamp described in the companion paper, where the uncertainties related to calibration factors are also discussed in detail (Gómez Martin et al., 2010).

Both I_2 and I also showed an anti-correlation with tidal height during daytime (i.e. higher mixing ratios at low tide), except on 2 May, where no strong anti-correlation was noticeable (Fig. 2a and b). Note that the gaps in the I_2 and I dataset correspond to periods of rainfall.

Bursts in the total number of ultrafine aerosols, between 3–9 nm in diameter, were observed only during daytime and low tide on 5 days (Fig. 2c). The highest concentration of ultrafine particles measured was $(1.8\pm0.3)\times10^4$ particles cm^{-3}, on 2 May. The background concentration of ultrafine particles was $(1.7\pm0.1)\times10^3$ particles cm^{-3}. During low tide, there was no change in the concentrations of aerosol with diameter >30 nm, indicating that the burst was only in the nucleation mode. The mean particle formation rate observed was 2.6±0.8 cm^{-3} s^{-1}, and the growth rate ranged from 1 to 8 nm h^{-1} (calculated using the method described by Birmili et al., 2003). The SMPS-observed size distributions show the growth of these particles where the maximum diameter ranged from 14-25 nm. A classic 'banana' shaped particle growth event was not observed, as shown in Fig. 3. Interestingly, high concentrations of ultrafine particles were also observed even when the I_2 and I mixing ratios did not show a large increase,

ACPD
10, 27227–27253, 2010

e.g. 2nd, 4 and 5 May (Fig. 2a, b and c). During the last four days, the integrated observed particle number was correlated to the tidal amplitude (Fig. 2c). In contrast, on 30 April and 1 May, the integrated particle number does not follow the same pattern.

Figure 2d shows the O_3, NO and NO_2 data throughout the campaign. The O_3 mixing ratios were variable with values ranging between ~15 and ~70 ppbv (equivalent to nmol mol^{-1}), with an average of about 50 ppbv. The NO and NO_2 also showed large variability during the campaign with NO_2 mixing ratios averaging ~2 ppbv during daytime low tide conditions. Wind speed and direction during the time of observations is shown in Fig. 2e. On average, the wind speed was higher during daytime compared to the night time, and showed significant day-to-day variability throughout the campaign. Low wind speeds of about 1–5 m s^{-1} were observed during low tide on 30 April–2 May, while higher speeds, between about 7–9 m s^{-1}, on 3–5 May. Note that there was no correlation between wind speed and I ($R^2 = 0.095$), I_2 ($R^2 = 0.063$) or ultrafine particles ($R^2 = 0.0032$). However, the wind direction was always within a sector of ±30° northward, which most of the time passed over the island of Arosa (Fig. 2e). Solar radiation data was not available through the campaign, although the conditions were variable with some days being overcast with a near continuous presence of clouds.

4 Discussion

The fact that I_2, I and ultra-fine particles show a strong tidal signature indicates that sources for all three are similar. The source is most probably exposure of macroalgae, which induces emission of I_2, ultimately leading to formation of iodine oxide particles as has been reported in the past (O'Dowd et al., 2002; Saiz-Lopez et al., 2006; McFiggans et al., 2010). As mentioned above, a macroalgal belt, 30-50 m wide, was observed within the intertidal zone adjacent to the measurement site along the coast. The species *Laminaria hyperborea*, which is known to be a strong emitter of I_2 (Ball et al., 2010) was widely noticeable within this macroalgal belt. The presence of laminaria forests along the Galician coast is well documented (Pérez-Ruzafa et al., 2003). Along

ACPD
10, 27227–27253, 2010

with *Laminaria hyperborea, Laminaria ochroleuca* was also present in large quantities. This species was shown to be an I_2 emitter by direct exposure of samples collected from the intertidal pool to the ROFLEX (Gómez Martin et al., 2010). Furthermore, the contribution of additional iodine emissions from the second belt of macroalgae to the north of the measurement site at a distance of 3–4 km near the island of Arosa, or a possible third injection point at the other side of the bay at a distance of 15-20 km cannot be ruled out. The wind direction throughout the campaign indicates that the air mass had passed over both these potential iodine sources.

An I_2 peak mixing ratio of 350±100 pptv is one of the highest daytime observations reported to date. In the past, studies at other coastal locations have reported a daytime maximum of 25–29 pptv through integrated long-path differential optical absorption spectroscopy (LP-DOAS) measurements at Mace Head (Saiz-Lopez and Plane, 2004; Huang et al., 2010), 115 pptv using in situ measurements at Mace Head (Saiz-Lopez et al., 2006), 87 pptv at Mweenish Bay-I and 302 pptv Mweenish Bay-II, both close to Mace Head using in situ techniques (Huang et al., 2010), 32 pptv (integrated) and 50 pptv (in situ) at Roscoff (Mahajan et al., 2009; McFiggans et al., 2010), and 3 pptv (in situ) at Scripps Pier, La Jolla, California (Finley and Saltzman, 2008). The peak I atom mixing ratio of 10±5 pptv is lower than a peak of 22 pptv reported by Bale et al. (2008) at Mace Head. Throughout the campaign the average daytime I_2/I ratio ranged between 20–40, with an average value of 32. In the past, studies in a similar semi-polluted environment such as Roscoff have indicated much lower I_2/I ratios, peaking at ~2 at a height of 4–6 m, where the I atom concentration was modelled from IO observations (Mahajan et al., 2009). A model study by Saiz-Lopez et al. (2006) at Mace Head, which is a cleaner environment with respect to NO_x, predicted an I_2/I ratio of ~5 at a height of 5 m during the daytime; this was later confirmed through I atom measurements made by Bale et al. (2008).

On 3 days (2, 4 and 5 May) when ultrafine particle bursts were measured, the gas-phase iodine species did not show an increase (Fig. 2 a, b and c). Similarly, on 30 April, I and I_2 were elevated during low tide, but the ultrafine particles did not show a large

ACPD
10, 27227–27253, 2010

increase over the background concentrations. However, it should be noted that on 30 April, the NO_2 and NO mixing ratios were larger than the rest of the campaign, with an average [NO_2] of 8 ppbv, about 4 times the average on other days. The source of this high NO_x is most probably relatively fresh pollution as the total aerosol surface area on this day was not significantly higher than the campaign average. The dependence of iodine oxides on NO_x levels is discussed in detail in Sect. 4.3.

The absence of a strong correlation between the gas-phase iodine species and the ultrafine particles indicates that although the sources of both are dependent on tidal height, they are not from the same location.

Hence, there are two outstanding questions regarding the observations: (i) the high I_2:I ratio of ~32; and (ii) the absence of a strong correlation between ultrafine particles and the measured iodine species.

We use the one dimensional photochemistry and transport Tropospheric Halogen Chemistry Model (THAMO) (Saiz-Lopez et al., 2008) to address these two questions. The iodine chemistry scheme utilised in this work has been updated following Mahajan et al. (2009). The rates of photolysis for all the species are calculated on-line using an explicit two-stream radiation scheme from (Thompson, 1984). The 1-D model is used with a vertical resolution of 10 cm and a boundary layer height of 1 km. The concentrations of all the iodine species, O_3 and NO_x are allowed to vary. The model was initialised with [NO_2] = 2 ppbv and aerosol surface area = 6×10^{-7} cm^2 cm^{-3} (typical of measurements made during the LEGOLAS campaign). The midday values for HO_2 and OH were set to 6 and 0.1 pptv, respectively, according to past observations in the mid-latitudinal MBL (Smith et al., 2006). Considering that the macroalgal belt was approximately 40 m in width, an air mass passing over the exposed macroalgae would take 10 s at 4 m s^{-1} or 5 s at 8 m s^{-1}, which were the average wind speeds on 30 April and 3rd May when high mixing ratios of I and I_2 were observed. The model results were found to be sensitive to two parameters: the eddy diffusion coefficient (K_z) and the rates of photolysis, which are discussed in Sect. 4.1.

ACPD
10, 27227–27253, 2010

The high I_2/I ratio indicates that the source for I_2 and I is local, most probably from the macroalgal bed observed adjacent to the measurement site, due to the short life time of I_2 (6 s for clear sky conditions). However, the particles would not have enough time to form within the transport time of up to 10 s and hence a second injection point is necessary to explain the observed ultrafine particle bursts. This second injection point could be at 3-4 km near the island of Arosa, where a similar macroalgal belt was observed, or further north about 15–20 km away near the coast of Cabo de Cruz.

4.1 I_2/I ratio

First, we run the model with a single injection point close to the measurement location to test under what conditions the local emissions can account for the I_2/I ratio. We consider two possible explanations for the ratio, first, increased vertical mixing of I_2 along with reduced photolysis; and second, an extra chemical removal of I atoms.

For the first condition, using only changes to vertical mixing and rates of photolysis, we ran the model for four scenarios. In scenario 1, K_z is calculated using the wind speed data and a surface roughness length of 1 cm, according to a vertical transport parameterisation by Stull (1988) which is described in Saiz-Lopez et al. (2008). K_z ranges from 1×10^3 cm^2 s^{-1} close to the surface to 4×10^4 cm^2 s^{-1} at 20 m in the boundary layer. For scenario 1, photolysis rates are calculated for clear sky conditions. In scenario 2, vertical mixing is the same as in scenario 1, but the photolysis rates are calculated for 50% cloudy conditions. For scenario 3, faster vertical mixing is considered close to the surface, with K_z ranging from 1×10^4 cm^2 s^{-1} close to the surface to 7×10^4 cm^2 s^{-1} at 20 m and clear sky conditions. Finally, in scenario 4, vertical mixing is the same as scenario 3 along with 50% cloud cover, to reflect the overcast conditions during some days of the campaign. To reproduce the absolute levels of I_2, a flux of 1.2×10^{13} molecule cm^{-2} is required lasting for 10 seconds to simulate the passing of an air mass over the macroalgal belt.

ACPD
10, 27227–27253, 2010

Figure 4 shows the I_2/I ratio predicted by the model for the above 4 scenarios. The average observed ratio of ~32 cannot be reproduced for scenario 1, 2 or 3. An increase in vertical mixing helps the emitted I_2 to mix up to the measurement height of 1.5 m (i.e. height of the ROFLEX measurements). To reach a ratio of ~32, using only an increase in vertical mixing, the K_z near the surface needs to be as high as 1×10^7 cm^2 s^{-1}, meaning that an air mass at the surface would take only 5 second to rise up to 100 m, which is unrealistic. Therefore, the observed I_2/I ratio cannot be reproduced using only an increase in vertical mixing. If we consider only a decrease in the rate of photolysis, without an increase in the vertical mixing by changing the cloud cover to even more than scenario 3 to 80%, the model predicts much higher levels of I_2 close to the source. In this case, a lower flux of 3.0×10^{12} molecule cm^{-2} is necessary to reproduce the absolute levels of I_2 (~350 pptv) due to the longer lifetime of I_2. However, the absolute levels of I and the observed ratio are reproduced after 20 s in the model, which is twice as long as the travel time the air mass would take to reach the measurement site, even under low wind speed conditions. Hence, scenario 4, which reproduces the observations and absolute levels of I and I_2 after 10 s of transit time, is a possible scenario to account for the observed I_2/I ratio. The model predicts peak mixing ratios of 322 pptv and 9.7 pptv for I_2 and I, respectively, after 10 s, which is in good agreement with the observations (Fig. 2a, b).

Now we consider whether the I_2/I ratio can be explained using chemical removal of I atoms through reaction with an unknown species. We define Scenario 5, with vertical mixing and photolysis rates calculated similar to Scenario 1, but with an extra species prescribed to react with I atoms with a rate constant of of 1×10^{10} cm^3 molecule^{-1} s^{-1} (i.e., close to the collision frequency), thereby setting a lower limit to the concentration of this species. This concentration is then tuned to reproduce the observations. In Scenario 5, an I_2 flux of 5.4×10^{12} molecule cm^{-2}, along with 1.5 ppbv of the unknown species is required to reproduce the I_2/I ratio of ~32 (Fig. 4) along with 335 pptv of I_2 and 10.5 pptv of I after 10 s, which are in good agreement with the observations. The identity of an organic species or group of species reacting with I is difficult to assess.

ACPD
10, 27227–27253, 2010

Iodine atoms are generally not very reactive with organic compounds (NIST, 2010). They are unable to abstract H atoms from saturated hydrocarbons, e.g. the reaction of I atoms with a major organic species like methane has a large activation energy of $E_A = 140$ kJ mol^{-1}, which effectively prevents the reaction from proceeding at ambient temperatures. Addition to double bonds of unsaturated hydrocarbons does not seem to be very efficient either (e.g. for I + propylene, $E_A = 75$ kJ mol^{-1}), although reaction with longer chain unsaturated hydrocarbons like isoprene have not been studied to date. Reactions with atmospherically relevant halo-alkanes, alcohols and aldehydes also have high activation energies. Radical-radical reactions (e.g. with methoxy, methyl peroxy, allyl) are fast, but such radicals are not expected to be at the high concentrations required by the model simulation. Note that the first-order removal rate for such a chemical sink must be approximately twice as fast as the combined rate of reaction of iodine atoms with O_3 and NO_x to explain the observed I_2/I ratio. Such a chemical sink could possibly result from a combination of reactions with a mixture of organics produced by the interaction of marine air masses, forest emissions from the island of Arosa and anthropogenic pollution.

4.2 Ultra-fine particles

The mechanism of iodine-induced nucleation has been the subject of intense research during the last few years (Burkholder et al., 2004; O'Dowd and Hoffmann, 2005; Saunders and Plane, 2005; Pechtl et al., 2006; Saunders and Plane, 2006; Saunders et al., 2010), but there are still some outstanding questions. Recent laboratory (Saunders et al., 2010) and modelling (Mahajan et al., 2010) studies indicate that I_2O_3 and I_2O_4 monomers rather than I_2O_5 are more likely to be responsible for formation of iodine oxide particles. Thus the sum of I_2O_3+I_2O_4 can be considered as a good indicator for the total condensable mass available for iodine induced nucleation.

In scenario 4 and 5, both of which reproduce the observed I_2/I ratio after 10 s, the model predicts only 1×10^{-3} pptv and 1×10^{-5} pptv, respectively, of I_2O_3 + I_2O_4 at 3.5 m (the height of measurements for ultrafine particles during the LEGOLAS study), which

ACPD
10, 27227–27253, 2010

is equivalent to only 28 particles cm^{-3} and 0.28 particles cm^{-3} of diameter 7 nm, which we take to represent the average diameter for iodine oxide particles in a range of 3–9 nm. In this calculation we employ a particle density of 2 g cm^{-3} for hydrated iodine oxide particles (Saunders et al., 2010). This would not be enough to reproduce particle bursts of up to 1.8×10^4 particles cm^{-3}, which were observed during the campaign. In addition, there is a lack of correlation between the ultrafine particles and I ($R^2 = 0.02$) and I_2 ($R^2 = 0.02$), with the absence of a particle burst in the presence of elevated I and I_2 on 30 April and the absence of elevated I and I_2 in the presence of particle bursts on 2, 4 and 5 May. This indicates that the macroalgal belt close to the measurement site was not the source for the observed ultrafine aerosols but a second injection point, which does not contribute to the I and I_2 observations is the source for the particles. If the second macroalgal belt close to the island of Arosa (~3.5 km distance, Figure 1) was the source of these particles, the air mass passing over this source would have reached the measurement site between 8-15 min later depending on the wind speed. If the injection had taken place at the other side of the bay, close to Cabo de Cruz (~15 km distance, Fig. 1), then the air mass would take approximately 60 min to reach the measurement site.

In scenario 4, where the observations are reproduced using only high K_z and low photolysis, the model predicts that $I_2O_3+I_2O_4$ would have been ~22 pptv at the height of measurement (3.5 m) when the air mass reached the measurement site after 12 min. This corresponds to $\sim8\times10^5$ particles cm^{-3} of diameter 7 nm. This particle number density is much higher than the observed maximum of 1.8×10^4 particles cm^{-3}. In addition, the model also predicts up to 40 pptv of I_2 and 36 pptv of I atoms at 1.5 m, which was not observed by ROFLEX. If we reduce the flux from this second injection point to 2×10^{12} molecule cm^{-2}, i.e. about 10 times lower, the model predicts $\sim2\times10^4$ particles cm^{-3} after 12 min, which is in good agreement with the observations. However, the model also predicts about 9 pptv of I atoms, which was not observed by the ROFLEX whenever particle bursts were observed. Hence the I, I_2 and particle observations cannot be reproduced in scenario 4, even with a lower flux if the second

ACPD
10, 27227–27253, 2010

injection point is at the island of Arosa at a distance of 3.5 km. In contrast, if the second injection point in this scenario is in fact at the other end of the bay near Cabo de Cruz, the model predicts ~1 pptv of I atoms, ~1.1 pptv of I_2 and ~1 pptv of I_2O_3+I_2O_4 after 60 min. Thus, the I and I_2 would be under the detection limit of the instrument when the air mass from the second injection point reaches the observations site, while 1 pptv of I_2O_3+I_2O_4 corresponds to ~2.8×10^4 particles cm^{-3} of diameter 7 nm, which is in good agreement with the observations. The reduction in the I_2O_3+I_2O_4 in this case is due to uptake on background aerosols and dilution in the vertical column, although the vertical dilution is subject to large uncertainties over 1 h of transport time. The I, I_2 and I_2O_3+I_2O_4 distributions in scenario 4 using a second injection point at a distance of 15 km is shown in Fig. 5 (panels a, b and c). Note however that in this scenario, an injection point at the Island of Arosa is not considered in order to reproduce the I/I_2 ratio and the particles are produced using an injection point at 15 km, while the ratio is produced using a local source.

In scenario 5, if we consider that the second injection point is at the island of Arosa rather than 15 km away, the model predicts only ~1×10^{-5} pptv of I, 2×10^{-5} pptv of I_2 and only 0.1 pptv of I_2O_3+I_2O_4 after 12 min. This corresponds to ~2.8×10^3 particles cm^{-3}, which is much lower than the observed maximum of 1.8×10^4 particles cm^{-3}. If we increase the I_2 flux to 1.8×10^{13} molecule cm^{-2}, or use the same flux of 1.2×10^{13} molecule cm^{-2} for a longer time of 15 s (macroalgae emission area ~60 m wide), the model now predicts about 1×10^{-4} pptv of I, 2×10^{-4} pptv of I_2 and 0.6 pptv of I_2O_3+I_2O_4 corresponding to ~1.7×10^4 particles cm^{-3} of 7 nm diameter. In addition, the predicted values of I and I_2 resulting from the injection point 3.5 km away would be well under the detection limit of the ROFLEX (2 pptv for I and 30 pptv for I_2) and the I_2/I ratio would be determined only by the local source. The I, I_2 and I_2O_3+I_2O_4 vertical distributions for scenario 5 are presented in Fig. 5 (panels d, e and f).

Thus the I_2/I ratio and ultrafine particle observations can be reproduced in both scenarios by considering different sources for the particles, in scenario 4 at 15 km distance, while in scenario 5, at 3.5 km. It should, however, be noted that the number of particles

ACPD
10, 27227–27253, 2010

predicted are indicative of the total condensable mass from iodine species and we do not model the particle distribution for a direct comparison with the particle observations.

While no information about macroalgal distribution around Cabo de Cruz was available, a marcroalgal distribution around the island of Arosa was noticeable. However, none of the scenarios offer a definitive conclusion on the iodine emission source, or the main causes for the high I_2/I ratio. It is possible that there was a combination of the above two scenarios with vertical mixing, low photolysis and a reaction with some unknown compound acting simultaneously.

4.3 Iodine oxide dependence on NO_x

On 30 April, the highest levels of I and I_2 over the campaign were observed, but there is a distinct lack of a large particle burst compared to the other days of measurements. Since the wind speed and wind direction are comparable to days when particle bursts were observed (Fig. 2c and e), the effect of meteorological factors can be discounted. However, on this day the NO_2 averages about 8 ppbv during low tide, which is much higher than the average of 2 ppbv during the rest of the campaign, indicating that iodine-NO_x chemistry is most probably the reason for the absence of ultrafine particle formation on this occasion. Recently, it has been suggested that iodine chemistry is self sustaining in semi-polluted environments due to a mechanism which recycles the reservoir species $IONO_2$ through the reaction $IONO_2 + I \rightarrow I_2 + NO_3$ (Mahajan et al., 2009), with a rate constant of 5.5×10^{-11} cm^3 molecule^{-1} s^{-1} at 290 K (Kaltsoyannis and Plane, 2008). However, at large NO_2 values this reaction is unable to compete with the reaction of $IO + NO_2 + M \rightarrow IONO_2 + M$ (3.8×10^{-12} cm^3 molecule^{-1} s^{-1} at 290 K and 1 atm; Atkinson et al., 2007). In addition, NO_x also slows down the formation of higher iodine oxides through other reactions such as $I + NO_2 + M \rightarrow INO_2 + M$ (5.4×10^{-12} molecule^{-1} s^{-1} at 290 K and 1 atm), $IO + NO \rightarrow I + NO_2$ (1.95×10^{-11} molecule^{-1} s^{-1} at 290 K) (Atkinson et al., 2007) and, $OIO + NO \rightarrow IO + NO_2$ (6.7×10^{12} molecule^{-1} s^{-1} at 290 K) (Plane et al., 2006).

ACPD
10, 27227–27253, 2010

We now run THAMO under Scenarios 4 and 5 with a single injection point while varying the NO_x mixing ratio to see under what conditions particle formation would be possible. Figure 6 shows the dependence of IO, OIO, $IONO_2$ (at a height of 1.5 m), and I_2O_3+I_2O_4 (at a height of 3.5), on the NO_x levels. This simulation shows that iodine chemistry is strongly influenced by the NO_x mixing ratio, with only about 0.2 pptv and 0.1 pptv of I_2O_3+I_2O_4 predicted after 60 min in scenario 4 and 12 min in scenario 5, respectively, in the presence of 8 ppbv NO_x. This corresponds to only $\sim 5.6\times10^3$ particles cm^{-3} and $\sim 2.8\times10^3$ particles cm^{-3} of diameter 7 nm, indicating that a large particle burst would not be seen in the presence of high NO_x, as was observed on 30 April. Additionally, the observation of elevated levels of I and I_2 on this day provides further evidence for the I and I_2 observations being a local phenomenon compared to the ultrafine particles, which are most probably emitted further away from the measurement site.

Potential interferences in the ROFLEX observations which could have affected the I_2/I ratio have been dealt with in detail in the companion paper (Gómez Martin et al., 2010). Aerosol or water deposition on fluorescence collection optics could also affect the relative sensitivity, although noticeable deposits on optical surfaces were not observed when the fluorescence cell was taken apart after the campaign. Relative intensity changes of the different atomic iodine lines contributing to excitation of I and I_2 could result in a more effective excitation of I_2 during the campaign compared to the calibration measurements. For instance, a 2 fold lost of sensitivity towards I or enhancement of sensitivity towards I_2 could bring the I_2/I ratio to levels explainable without invoking increased vertical mixing or an extra I atom sink. Such changes have not been observed so far in an undergoing long term measurement, where the ratio of sensitivities towards I and I_2 stays fairly constant after about a month. However, since lamp aging effects where observed towards the end of the campaign (Gómez Martin et al., 2010), such possibility cannot be entirely ruled out.

ACPD
10, 27227–27253, 2010

5 Summary and conclusions

We report the first concurrent observations of I, I_2 and ultrafine particles in a coastal environment, which contribute to expand geographically the relatively small available dataset of iodine, especially in semi-polluted environments. The complexity of the measurement location is shown by the lack of correlation between I_2/I and ultrafine particles, indicating that although the source for all three is tidal in nature, it is not at the same location. In addition, a high I_2/I ratio was observed throughout the campaign, which can be explained by a combination of high vertical mixing close to the surface and lower photolysis, or through the chemical loss of I atoms by reaction with an unknown species, or a combination of the three. The I, I_2 and ultrafine particle observations can be reproduced in the model using two injection points, one very close to the measurement site and a second about 1 hour upwind or 12 min upwind. Further concurrent measurements of I, I_2 and ultrafine particles, and other RIS, in semi-polluted environments are needed to confirm the high I_2/I ratio and to improve our understanding of the role of iodine in such chemically complex semi-polluted conditions.

Acknowledgements. The authors are grateful to T. Ingham for helpful discussions. We thank Aostreria S. L. and the Council of O Grove for logistical support. The Spanish Research Council (CSIC), the Regional Government of Castilla-La Mancha (FGMACLM), Spain, and University of Leeds, UK funded this work.

References

Alicke, B., Hebestreit, K., Stutz, J., and Platt, U.: Iodine oxide in the marine boundary layer, Nature, 397, 572–573, 1999.

Allan, B. J., Plane, J. M. C., and McFiggans, G.: Observations of OIO in the remote marine boundary layer, Geophys. Res. Lett., 28, 1945–1948, 2001.

Atkinson, R., Baulch, D. L., Cox, R. A., Crowley, J. N., Hampson, R. F., Hynes, R. G., Jenkin, M. E., Rossi, M. J., and Troe, J.: Evaluated kinetic and photochemical data for atmospheric

ACPD

10, 27227–27253, 2010

chemistry: Volume III – gas phase reactions of inorganic halogens, Atmos. Chem. Phys., 7, 981–1191, doi:10.5194/acp-1-981-2007, 2007.

Bale, C. S. E., Ingham, T., Commane, R., Heard, D. E., and Bloss, W. J.: Novel measurements of atmospheric iodine species by resonance fluorescence, J. Atmos. Chem., 60, 51–70, 2008.

Ball, S. M., Hollingsworth, A. M., Humbles, J., Leblanc, C., Potin, P., and McFiggans, G.: Spectroscopic studies of molecular iodine emitted into the gas phase by seaweed, Atmos. Chem. Phys., 10, 6237–6254, doi:10.5194/acp-10-6237-2010, 2010.

Birmili, W., Berresheim, H., Plass-Dülmer, C., Elste, T., Gilge, S., Wiedensohler, A., and Uhrner, U.: The Hohenpeissenberg aerosol formation experiment (HAFEX): a long-term study including size-resolved aerosol, H2SO4, OH, and monoterpenes measurements, Atmos. Chem. Phys., 3, 361–376, doi:10.5194/acp-3-361-2003, 2003.

Bloss, W. J., Lee, J. D., Johnson, G. P., Sommariva, R., Heard, D. E., Saiz-Lopez, A., Plane, J. M. C., McFiggans, G., Coe, H., Flynn, M., Williams, P., Rickard, A. R., and Fleming, Z. L.: Impact of halogen monoxide chemistry upon boundary layer OH and HO_2 concentrations at a coastal site, Geophys. Res. Lett., 32, L06814, doi:10.1029/2004GL022084, 2005.

Burkholder, J. B., Curtius, J., Ravishankara, A. R., and Lovejoy, E. R.: Laboratory studies of the homogeneous nucleation of iodine oxides, Atmos. Chem. Phys., 4, 19–34, doi:10.5194/acp-4-19-2004, 2004.

Chameides, W. L. and Davis, D.: Iodine: Its Possible Role in Tropospheric Photochemistry, J. Geophys. Res., 85, 7383-7398, 1980.

Davis, D., Crawford, J., Liu, S., McKeen, S., Bandy, A., Thornton, D., Rowland, F., and Blake, D.: Potential impact of iodine on tropospheric levels of ozone and other critical oxidants, J. Geophys. Res.-Atmospheres, 101, 2135–2147, 1996.

Finley, B. D. and Saltzman, E. S.: Observations of Cl_2, Br_2, and I_2 in coastal marine air, J. Geophys. Res., 113, doi:10.1029/2008JD010269, doi:10.1029/2008JD010269, 2008.

Gómez Martin, J. C., Blahins, J., Gross, U., Ingham, T., Goddard, A., Mahajan, A. S., Ubelis, A., and Saiz-Lopez, A.: In situ detection of atomic and molecular iodine using resonance and off-resonance fluorescence by lamp excitation: ROFLEX, Atmos. Meas. Tech. Discuss., 3, 3803-3849, doi:10.5194/amtd-3-3803-2010, 2010.

Huang, R.-J., Seitz, K., Buxmann, J., Pöhler, D., Hornsby, K. E., Carpenter, L. J., Platt, U., and Hoffmann, T.: In situ measurements of molecular iodine in the marine boundary layer: the link to macroalgae and the implications for O_3, IO, OIO and NO_x, Atmos. Chem. Phys., 10,

ACPD

10, 27227–27253, 2010

4823–4833, doi:10.5194/acp-10-4823-2010, 2010.
Kaltsoyannis, N. and Plane, J. M. C.: Quantum chemical calculations on a selection of iodine-containing species (IO, OIO, INO_3, (IO)(2), I_2O_3, I_2O_4 and I_2O_5) of importance in the atmosphere, Phys. Chem. Chem. Phys., 10, 1723–1733, 2008.
Leigh, R. J., Ball, S. M., Whitehead, J., Leblanc, C., Shillings, A. J. L., Mahajan, A. S., Oetjen, H., Dorsey, J. R., Gallagher, M., Jones, R. L., Plane, J. M. C., Potin, P., and McFiggans, G.: Measurements and modelling of molecular iodine emissions, transport and photodestruction in the coastal region around Roscoff, Atmos. Chem. Phys. Discuss., 9, 21165–21198, doi:10.5194/acpd-9-21165-2009, 2009.
Mahajan, A. S., Oetjen, H., Saiz-Lopez, A., Lee, J. D., McFiggans, G. B., and Plane, J. M. C.: Reactive iodine species in a semi-polluted environment, Geophys. Res. Lett., 36, L16803, doi:10.1029/2009GL038018, 2009.
Mahajan, A. S., Plane, J. M. C., Oetjen, H., Mendes, L., Saunders, R. W., Saiz-Lopez, A., Jones, C. E., Carpenter, L. J., and McFiggans, G. B.: Measurement and modelling of tropospheric reactive halogen species over the tropical Atlantic Ocean, Atmos. Chem. Phys., 10, 4611–4624, doi:10.5194/acp-10-4611-2010, 2010.
McFiggans, G., Plane, J. M. C., Allan, B. J., Carpenter, L. J., Coe, H., and O'Dowd, C.: A modeling study of iodine chemistry in the marine boundary layer, J. Geophys. Res.-Atmos., 105, 14371–14385, 2000.
McFiggans, G., Coe, H., Burgess, R., Allan, J., Cubison, M., Alfarra, M. R., Saunders, R., Saiz-Lopez, A., Plane, J. M. C., Wevill, D. J., Carpenter, L. J., Rickard, A. R., and Monks, P. S.: Direct evidence for coastal iodine particles from Laminaria macroalgae – linkage to emissions of molecular iodine, Atmos. Chem. Phys., 4, 701–713, 2004, http://www.atmos-chem-phys.net/4/701/2004/.
McFiggans, G.: Marine aerosols and iodine emissions, Nature, 433, p. E13, 2005.
McFiggans, G., Bale, C. S. E., Ball, S. M., Beames, J. M., Bloss, W. J., Carpenter, L. J., Dorsey, J., Dunk, R., Flynn, M. J., Furneaux, K. L., Gallagher, M. W., Heard, D. E., Hollingsworth, A. M., Hornsby, K., Ingham, T., Jones, C. E., Jones, R. L., Kramer, L. J., Langridge, J. M., Leblanc, C., LeCrane, J.-P., Lee, J. D., Leigh, R. J., Longley, I., Mahajan, A. S., Monks, P. S., Oetjen, H., Orr-Ewing, A. J., Plane, J. M. C., Potin, P., Shillings, A. J. L., Thomas, F., von Glasow, R., Wada, R., Whalley, L. K., and Whitehead, J. D.: Iodine-mediated coastal particle formation: an overview of the Reactive Halogens in the Marine Boundary Layer (RHaMBLe) Roscoff coastal study, Atmos. Chem. Phys., 10, 2975–2999, doi:10.5194/acp-10-2975-2010,

ACPD
10, 27227–27253, 2010

2010.
NIST: Chemical Kinetics Database on the Web Standard Reference Database 17, Version 7.0 (Web Version), National Institute of Standards and Technology (NIST), 2010.
O'Dowd, C. D., Jimenez, J. L., Bahreini, R., Flagan, R. C., Seinfeld, J. H., Hameri, K., Pirjola, L., Kulmala, M., Jennings, S. G., and Hoffmann, T.: Marine aerosol formation from biogenic iodine emissions, Nature, 417, 632–636, 2002.
O'Dowd, C. D., Facchini, M. C., Cavalli, F., Ceburnis, D., Mircea, M., Decesari, S., Fuzzi, S., Yoon, Y. J., and Putaud, J. P.: Biogenically driven organic contribution to marine aerosol, Nature, 431, 676–680, 2004.
O'Dowd, C. D., and Hoffmann, T.: Coastal new particle formation: A review of the current state-of-the-art, Environ. Chem., 2, 245–255, 2005.
Pechtl, S., Lovejoy, E. R., Burkholder, J. B., and von Glasow, R.: Modeling the possible role of iodine oxides in atmospheric new particle formation, Atmos. Chem. Phys., 6, 505-523, 1doi:10.5194/acp-6-505-2006, 2006.
Pérez-Ruzafa, I., Izquierdo, J.-L., Araújo, R., Souza-Pinto, I., Pereira, L., and Bárbara, I.: Distribution maps of marine algae from the Iberian Peninsula and the Balearic Islands. XVII. Laminaria rodriguezii Bornet and aditions to the distribution maps of L. hyperborea (Gunner.) Foslie, L. ochroleuca Bach. Pyl. and L. saccharina (L.) Lamour. (Laminariales, Fucophyceae), Botanica Complutensis, 27, 155–164, 2003.
Peters, C., Pechtl, S., Stutz, J., Hebestreit, K., Honninger, G., Heumann, K. G., Schwarz, A., Winterlik, J., and Platt, U.: Reactive and organic halogen species in three different European coastal environments, Atmos. Chem. Phys., 5, 3357–3375, doi:10.5194/acpd-5-3357-2005, 2005.
Plane, J. M. C., Joseph, D. M., Allan, B. J., Ashworth, S. H., and Francisco, J. S.: An Experimental and Theoretical Study of the Reactions OIO + NO and OIO + OH, J. Phys. Chem., 2006.
Saiz-Lopez, A. and Plane, J. M. C.: Novel iodine chemistry in the marine boundary layer, Geophys. Res. Lett., 31, L04112, doi:10.1029/2003GL019215, 2004.
Saiz-Lopez, A., Plane, J. M. C., McFiggans, G., Williams, P. I., Ball, S. M., Bitter, M., Jones, R. L., Hongwei, C., and Hoffmann, T.: Modelling molecular iodine emissions in a coastal marine environment: the link to new particle formation, Atmos. Chem. Phys., 6, 883–895, doi:10.5194/acpd-6-883-2006, 2006.
Saiz-Lopez, A., Plane, J. M. C., Mahajan, A. S., Anderson, P. S., Bauguitte, S. J. B., Jones, A.

ACPD
10, 27227–27253, 2010

E., Roscoe, H. K., Salmon, R. A., Bloss, W. J., Lee, J. D., and Heard, D. E.: On the vertical distribution of boundary layer halogens over coastal Antarctica: implications for O_3, HO_x, NO_x and the Hg lifetime, Atmos. Chem. Phys., 8, 887–900, doi:10.5194/acpd-8-887-2008, 2008.

Saunders, R. W. and Plane, J. M. C.: Formation pathways and composition of iodine oxide ultra-fine particles, Environ. Chem., 2, 299–303, 2005.

Saunders, R. W. and Plane, J. M. C.: Fractal growth modelling of I2O5 nanoparticles, J. Aerosol Sci., 37, 1737–1749, 2006.

Saunders, R. W., Kumar, R., Martin, J. C. G. m., Mahajan, A. S., Murray, B. J., and Plane, J. M. C.: Studies of the Formation and Growth of Aerosol from Molecular Iodine Precursor, Zeitschrift für Physikalische Chemie, 224, 1095–1117, doi:10.1524.zpch.2010.6143, 2010.

Smith, S. C., Lee, J. D., Bloss, W. J., Johnson, G. P., Ingham, T., and Heard, D. E.: Concentrations of OH and HO2 radicals during NAMBLEX: measurements and steady state analysis, Atmos. Chem. Phys., 6, 1435-1453, doi:10.5194/acpd-6-1435-2006, 2006.

Stull, R. B.: An introduction to boundary layer meteorology, Kluwer Academic Publishers, London, UK, 1988.

Thompson, A. M.: The effect of clouds on the photolysis rates and ozone formation in the unpolluted troposphere, J. Geophys. Res.-Atmos., 89, 1341–1349, 1984.

Vogt, R., Crutzen, P., and Sander, R.: A mechanism for halogen release from sea-salt aerosol in the remote marine boundary layer, Nature, 383, 327–330, 1996.

ACPD

10, 27227–27253, 2010

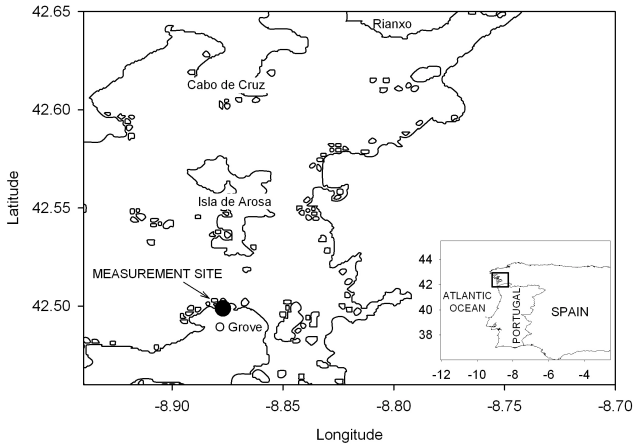

Fig. 1. Location of the measurement site during the LEGOLAS study. There is a macroalgae bed 30–50 m wide adjacent to the site within the inter-tidal zone. A similar bed occurs along the south coast of the island of Isla de Arosa (3 km). Information about macroalgal distribution to the north of the bay near Cabo de Cruz (15–20 km) was not available.

ACPD
10, 27227–27253, 2010

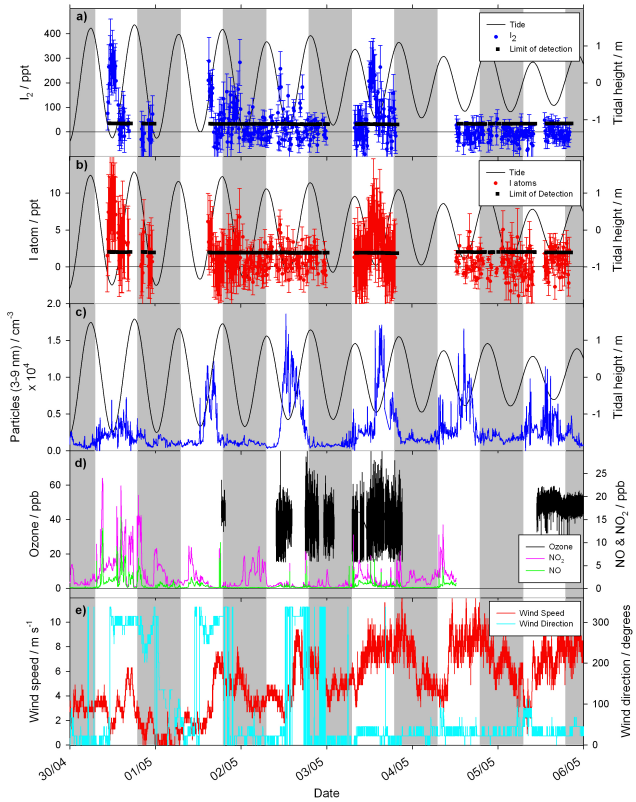

Fig. 2. Time series of measurements made during the LEGOLAS study. Panels **(a)**, **(b)** and **(c)** indicate the I_2, I and ultrafine particle observations along with the tidal variation. Panel **(d)** shows the O_3, NO and NO_2 observation, while the wind speed and direction is shown in panel **(e)**. Night time is shaded.

ACPD
10, 27227–27253, 2010

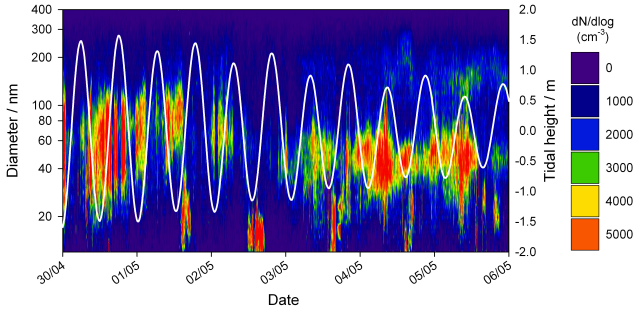

Fig. 3. SMPS observed particle distribution throughout the campaign. Classic "banana" shaped particle growth curves were not observed, with the maximum diameter for particle bursts ranging between 14–25 nm and the particle bursts were observed only during low tide day time conditions.

ACPD
10, 27227–27253, 2010

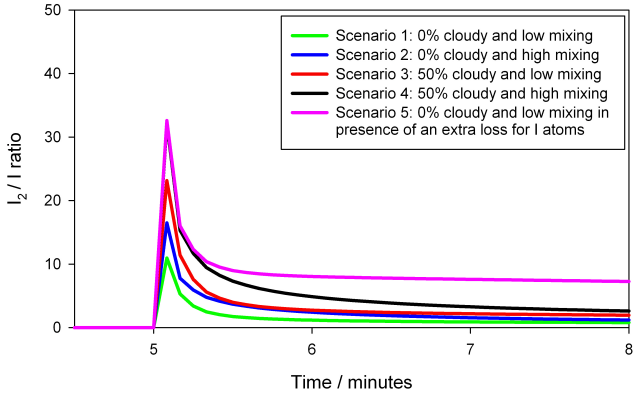

Fig. 4. I_2/I ratio change for five scenarios: (1) Photolysis is calculated with 0% cloud cover and slow vertical mixing close to the surface is considered, (2) 0% cloud cover with faster mixing close to the surface, (3) 50% cloud cover with slow mixing close to the surface, (4) 50% cloud cover, with fast mixing close to the surface and (5) 0% cloud cover with slow mixing close to the surface in the presence of an extra loss for I atoms through reaction with an unknown species.

ACPD
10, 27227–27253, 2010

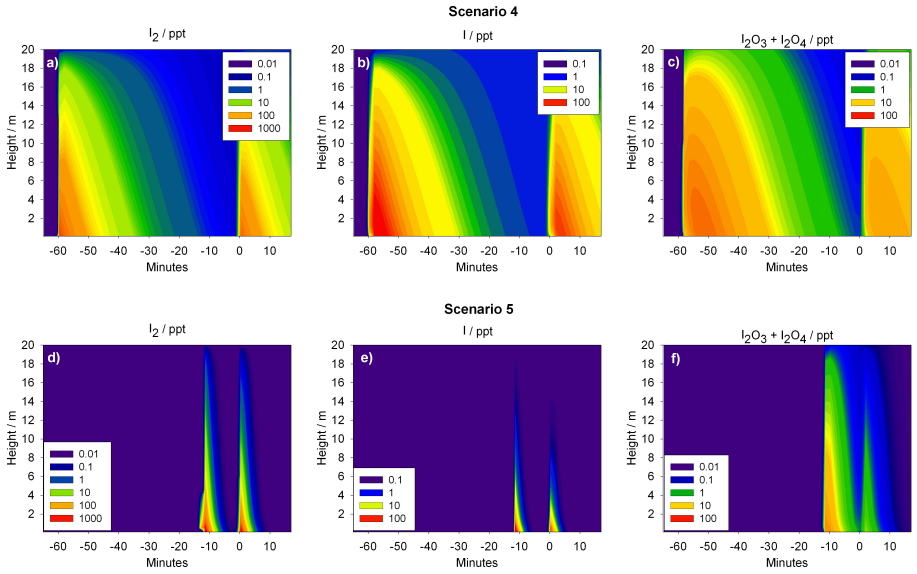

Fig. 5. Vertical distributions of **(a)** I_2, **(b)** I and **(c)** I_2O_3+I_2O_4 in scenario 4, with 50% cloud cover and fast mixing close to the surface and **(d)** I_2, **(e)** I and **(f)** I_2O_3+I_2O_4 in scenario 5 with an unknown chemical loss for I atoms. The air mass travelling over the bay arrives at the measurement site at time 0 with a local injection at −10 s. A second injection point is considered at −60 min for scenario 4 and −12 min for scenario.

ACPD
10, 27227–27253, 2010

Observations of atomic and molecular iodine and ultrafine particles

A. S. Mahajan et al.

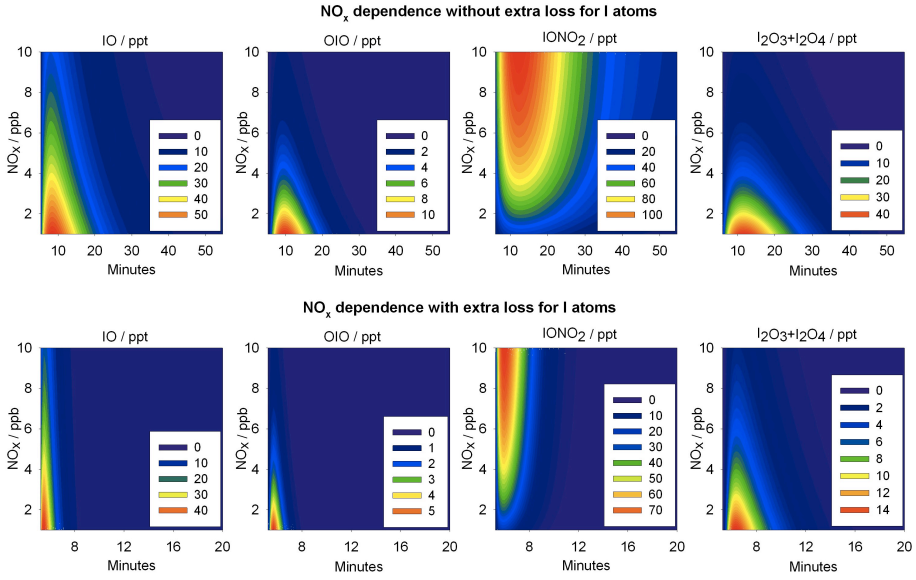

Fig. 6. Dependence of IO, OIO, $IONO_2$ and $I_2O_3+I_2O_4$ on NO_x mixing ratios for scenarios 4 and 5, which both reproduce the observed I_2/I ratio. Higher NO_x leads to lower levels of iodine oxides, with most of the iodine converted into $IONO_2$ as the reservoir species. The IO, OIO and $IONO_2$ are at a height of 1.5 m while the $I_2O_3+I_2O_4$ is at a height of 3.5 m. In the model injection of I_2 at a flux of 1.2×10^{13} molecule cm^{-2} takes place after 5 min for 10 s.

ACPD
10, 27227–27253, 2010